Chemical and gas-phase kinetics in a $CHF_3 + Ar$ discharge

Jakob P. Barz[1,2], Achim Lunk[2], and Christian Oehr[1]
[1] *Fraunhofer IGB, Stuttgart, Germany*
[2] *Institute for Plasma Research, University of Stuttgart, Stuttgart, Germany*

Abstract: The present work deals with experimental investigation as well as modeling of radical and metastable kinetics in a trifluoromethane/argon plasma. Therefore, space- and time-resolved laser-induced fluorescence measurements of the CF and CF_2 densities were carried out. For the interpretation of the observed glow and afterglow density data, the discharge was modeled from both the plasma kinetical and chemical point of view.

Keywords: fluorocarbon, laser-induced fluorescence, high resolution, plasma kinetics, chemical modeling

1 Introduction

Chemical plasmas, as used e.g. for etching, functionalization, or deposition, are highly complex. Reactive species are created by electron and ion impact-induced dissociation, by radiation processes, and by chemical reactions. The physical properties, in particular the discharge parameters, are fed back by the plasma-chemical reactions, and vice versa. Fluorocarbon plasmas are used in semiconductor processing and in coating technology. The plasma chemistry in these plasmas is quite complex: Both etching species and polymerizing species occur simultaneously. In addition, gas transport kinetics can be of importance as well, and can result in different kinds of radical-surface interactions. Due to the complexity, it is favorable to carry out both time-/space-resolved measurements and electrical/chemical simulations in order to assess the importance of different processes.

In a pulsed radio-frequency (r.f., 13.56 MHz) plasma of argon and trifluoromethane as used for thin-film deposition [1], laser-induced fluorescence (LIF) measurements were carried out to determine the spatiotemporal densities of CF and CF_2. The measurements were conducted with a high temporal and spatial resolution. In order to distinguish between electron-collision induced processes and chemical reactions, modeling of the plasma kinetics and the chemical processes was performed. Gas transport phenomena were considered as well.

2 Experimental Setup and Modeling

2.1 Plasma Generation

A capacitively coupled plasma (c.c.p.) of argon and trifluoromethane was ignited in a symmetric discharge chamber as depicted in figure 1. Power was supplied by a 13.56 MHz r.f. generator (Dressler Cesar), which was pulsed at 1-1000 Hz at duty-cycles (d.c.) of 10-100%. The d.c. is the ratio of pulse-on time to the total pulse duration. The gas flows and pressures were controlled by MKS mass flow and pressure controllers, respectively.

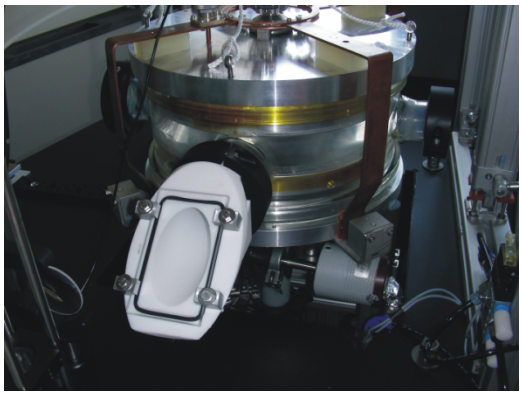

Figure 1: Symmetric ccp setup used for the investigations.

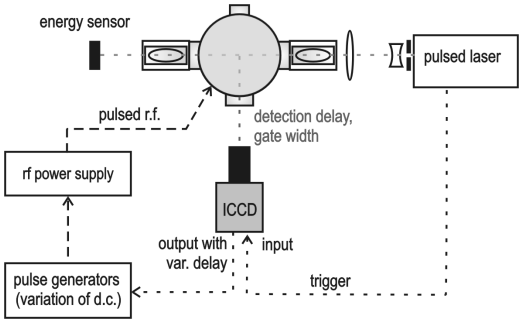

Figure 2: Setup of LIF. Here, axial profiles were acquired by binning.

2.2 Laser-induced fluorescence

In order to obtain highly-resolved density profiles, an Andor iStar ICCD camera was applied to monitor the fluorescence emission of laser-excited CF and CF_2

molecules. The excitations of the molecules were carried out in the A-X (1-0) and the A-X (0,11,0) transitions, respectively, by a frequency-doubled Nd-YAG pumped OPO system (Ekspla NT342-1-UV). The optical arrangement and the control setup are depicted in figure 2. In general, 2D fluorescence maps can be obtained by use of such a system (planar laser induced fluorescence, PLIF, see. e.g. [2, 3]). Due to the symmetric setup used here, the density of fluorescence emitters turned out to be laterally highly uniform, and to mainly only depend on the axial coordinate. Therefore, the ICCD was used in full binning mode. This mode is further referred to as linear laser-induced fluorescence (LLIF). The reduction of data compared to PLIF allows easier and faster evaluation of parameter studies. The setup was calibrated by conventional, zero-dimensional crossed-beam measurements. Further details are to be submitted.

2.3 Plasma Modeling

The collision processes as well as the chemical reactions taking place in the plasma were modeled with several different tools.

- The electron transport coefficients as well as the dissociation, ionization and attachment rate coefficients were determined with BOLSIG+, a two-term Boltzmann equation solver [4, 5]. As input data, the electron-collision cross sections according to Yanguas-Gil *et al.* [6] for argon, and according to Voloshin *et al.* [7] for trifluoromethane were applied.

- The electron-transport parameters as well as the ionization and attachment rate coefficients were used as input to the electrical discharge model. Modeling of the discharge was performed in SIGLO-RF [8, 9]. Such, amongst other parameters, the mean electron energy as well as the electron density were obtained. Together with the electron-energy dependent rate coefficients obtained in BOLSIG+, the overall fragmentation rates were calculated.

- The chemical model was set up in Comsol Multiphysics 4.5. The chemical reaction rate coefficients used were obtained from the literature [10–19]. The results of the previously mentioned models were included in this model. The role of several species, especially of atomic hydrogen and fluorine, is discussed in detail in [11].

To check the validity of the discharge model, the electron density and the current-voltage characteristics were measured. The results of the chemical model were compared to the LLIF data.

3 Results and Discussion

Time-resolved axial density profiles of CF and CF_2 are shown in figures 3 and 4 for 10 sccm CHF_3 flow in 60 sccm argon, 80 Pa pressure, 20 W peak power, and 35% dc in a 10 Hz pulsed plasma.

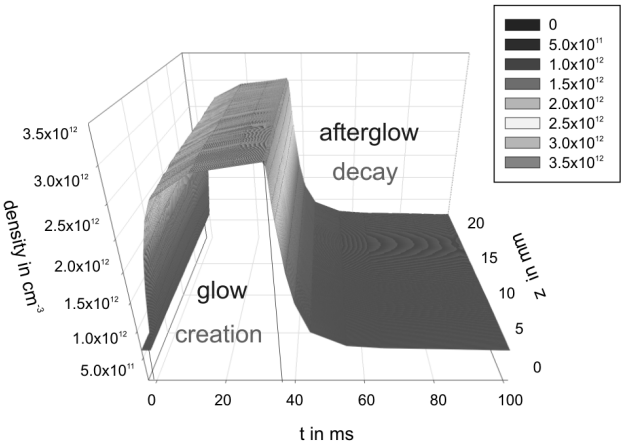

Figure 3: LLIF data of the CF density in temporal and axial resolution along a plasma pulse of 100 ms duration (35 ms on). Here, the axial data shown corresponds to have the reactor height.

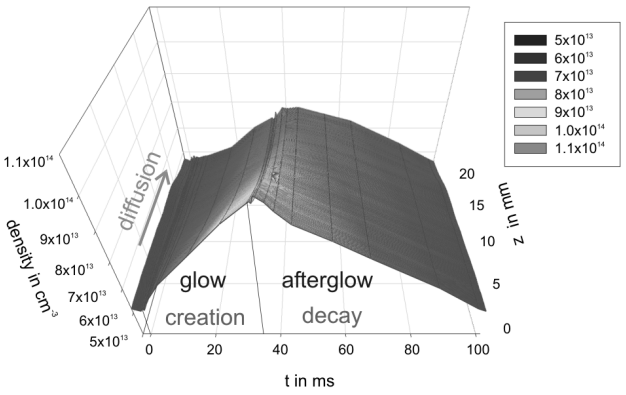

Figure 4: LLIF data of the CF_2 density in temporal and axial resolution along a plasma pulse of 100 ms duration (35 ms on). Here, the axial data shown corresponds to have the reactor height.

In both cases, an increase in density is observed after plasma ignition, which in the case of CF shows a saturation behavior. After switching off the discharge, CF shows a rapid decrease in concentration. The CF_2 density shows a short increase in density immediately after switching off the discharge, followed by an overall decay of the species.

A more detailed analysis on the temporal cross sec-

tions of the CF density shows that the concentration is always almost uniform in space. The fast increase in the early-glow regime will be discussed later. In the afterglow, the species disappears with a non-exponential function, which is due to several competing reactions taking place simultaneously.

The temporal-spatial development of the CF_2 density in figure 4 shows that the density is governed by a large axial anisotropy. This is discussed later on in this paper. The density increase in the early afterglow, immediately after switching off the discharge, can be attributed to a short net production, followed by depletion reactions. This observation is well documented and dicussed in the literature [20], and attributed to reactions of CF with F and CF_3 ($k_2 = 6.2 \times 10^{-15}\,\mathrm{cm^3 s^{-1}}$ and $10^{-11} - 10^{-10}\,\mathrm{cm^3 s^{-1}}$, respectively).

For the modeling of the processes in the plasma, it turned out that the electron-energy distribution functions are neither Maxwellian nor of Druyvsteyn-type, which is due to the presence of non-constant electron-collision cross sections. The mean electron energy in the discharge was calculated to be $\langle\epsilon\rangle = 5.6 - 5.8\,\mathrm{eV}$, the electron density was found to be $n_e = 7{\times}10^8\,\mathrm{cm^{-3}}$. The latter was confirmed by microwave interferometry. From these results, the overall fragmentation rates were determined. The most pronounced fragmentation channels due to electron impact are $CHF_3 \xrightarrow{e} CF_3 + H$ and $CHF_3 \xrightarrow{e} CHF_2 + F$ with rates k_1=0.075 s^{-1} and 0.04 s^{-1}, respectively.

A chemical model, not accounting for the anisotropic density of CF_2, was build based on these data. It was found to be in good agreement with a previous model from Voloshin *et al.* [16] under similar simulation conditions. However, experimentally, the peak $CF_{1/2}$ densities in the present experiment were about one order of magnitude larger than those predicted by the model.

From figure 4, we conclude that a strong wall production process for CF_2 exists during the plasma glow and in the early afterglow which should be considered in the model as well. The flux of molecules results in the pronounced axial, diffusion-related density profile. Such production processes are known to occur in diverse, mostly polymerizing plasmas [21–26], but the exact mechanisms are still a matter of discussion. Here, a maximum flux of $\Gamma_{CF_2} \approx 1 \times 10^{15}\,\mathrm{cm^{-2} s^{-1}}$ from the walls into the plasma is obtained from evaluation of the profile. This flux value is quite close to values determined by Sasaki *et al.* at a similar fluorine-to-hydrogen ratio in a CF_4/H_2 plasma [25].

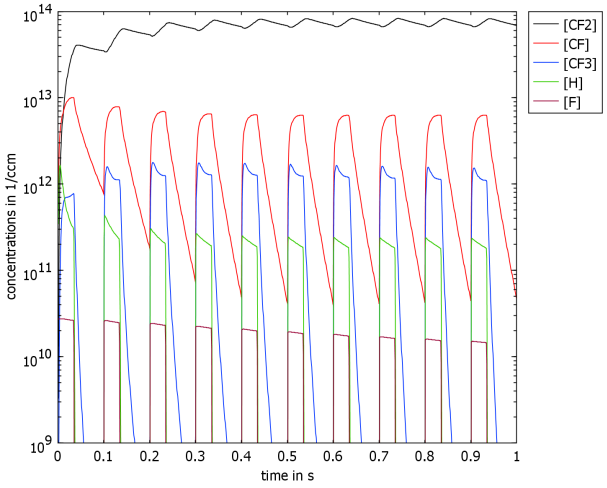

Figure 5: Densities of several low-molecular weight species in a plasma-pulse series of ten shots in the reactor center.

By adding the flux Γ_{CF_2} to the chemical model, a much better agreement between measured and modeled densities and profiles was achieved. In figure 5, the kinetics of several hydrofluorocarbon species, including H and F, are plotted. All concentrations increase at the beginning of the plasma pulse, and decrease after switching off the plasma. The modeled densities of CF and CF_2 agree with those obtained experimentally (figures 3 and 4). It is further observed that the concentrations of atomic hydrogen and fluorine are comparably small; this is due to their high reactivities, especially with hydrofluorocarbons.

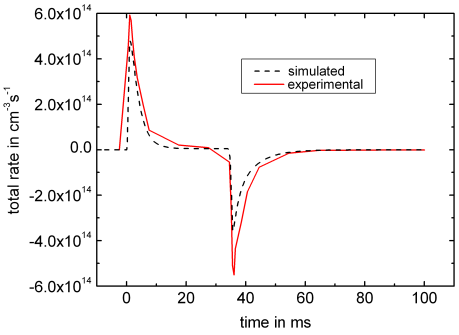

Figure 6: Experimental and modeled rates of CF production and dissipation.

Such, for example, the chemical model reveals that CF is mainly a product from the reaction $CF_2 + H \rightarrow CF + HF$ ($k_2 = 4.1 \times 10^{-11}\,\mathrm{cm^3 s^{-1}}$). The agreement in the rates between model and experiment is further depicted in figure 6: model rates were obtained from summing all chemical reaction channels involving CF either as a product or an educt. Compared to that, direct production of CF by fragmentation due to electron-impact on CHF_3 does not contribute sig-

nificantly, as the rate is two orders of magnitude too low ($k \approx 10^{12}\,\mathrm{cm^{-3}s^{-1}}$). This way, the steep increase in the CF density in the beginning of a plasma pulse seen in figure 3 can be attributed to chemical causes.

4 Summary and Conclusion

On the basis of electron-collision cross sections, the plasma kinetics of a fluorocarbon discharge were simulated. The major fragmentation channels were identified and introduced to a chemical model of the system. Such, the high-rate increases of CF_x species (x=1,2) as observed with an advanced laser-induced fluorescence method were related to (a) wall production in case of CF_2, and (b) purely chemical H-atom induced abstraction reactions in case of CF. Electron-collision induced fragmentation in the gas phase is found to be not a direct contributor to production of those two species, but yields e.g. the chemically highly important H-atoms. Finally, the plasma chemistry model shows excellent agreement with experimental data only in case that wall processes and diffusion are included.

References

[1] J. Barz, M. Haupt, U. Vohrer, H. Hilgers, and C. Oehr, Surface and Coatings Technology **200**, 453 (2005), PSE 2004.

[2] B. K. McMillin and M. R. Zachariah, Two-Dimensional Images of CF_2 Density in CF_4/Ar Plasmas by Laser-Induced Fluorescence in a GEC RF Reference Cell, in *IEEE TRANSACTIONS ON PLASMA SCIENCE* Vol. 24, pp. 113–114, 1996.

[3] M. R. Zachariah and B. K. McMillin, Solid State Technology **49**, 147 (1996).

[4] G. J. M. Hagelaar and L. C. Pitchford, Plasma Sources Science and Technology **14**, 722 (2005).

[5] G. Hagelaar and L. Pitchford, Bolsig+, online, www.laplace.univ-tlse.fr, 2008.

[6] Á. Yanguas-Gil, J. Cotrino, and L. L. Alves, Journal of Physics D: Applied Physics **38**, 1588 (2005).

[7] D. G. Voloshin, T. V. Rakhimova, K. S. Klopovskiy, and Y. A. Mankelevich, Journal of Physics: Conference Series **44**, 121 (2006).

[8] J. P. Boeuf and L. C. Pitchford, Phys. Rev. E **51**, 1376 (1995).

[9] Siglo-rf v.1.11, online, www.siglo-kinema.com, 1998.

[10] D. R. Burgess, M. R. Zacharaiah, W. Tsang, and P. R. Westmoreland, Progress in Energy and Combustion Science **21**, 453 (1995).

[11] M. J. Schabel, T. W. Peterson, and A. J. Muscat, Journal of Applied Physics **93**, 1389 (2003).

[12] I. Rozum, P. Limão-Vieira, S. Eden, J. Tennyson, and N. J. Mason, Journal of Physical and Chemical Reference Data **35**, 267 (2006).

[13] S. Rauf and M. J. Kushner, Journal of Applied Physics **82**, 2805 (1997).

[14] I. C. Plumb and K. R. Ryan, Plasma Chemistry and Plasma Processing **6**, 205 (1986).

[15] B. Dils, J. Vertommen, S. A. Carl, L. Vereecken, and J. Peeters, Phys . Chem. Chem. Phys. **7**, 1187 (2005).

[16] D. Voloshin *et al.*, IEEE Transactions on Plasma Science **35**, 1691 (2007).

[17] C. J. Ultee, Chemical Physics Letters **46**, 366 (1977).

[18] L. P. Walkauskas and F. Kaufman, Gas Phase Hydrogen Atom Recombination, in *Proc. 15th Symp. (Int.) on Combustion*, The Combustion Institute, Pittsburgh, 1975.

[19] J. Kerr and M. Parsonage, *Evaluated Kinetic Data on Gas Phase Addition Reactions. Reactions of Atoms and Radicals with Alkenes, Alkynes and Aromatic Compounds* (Butterworths, London, 1972).

[20] J. P. Booth, H. Abada, P. Chabert, and D. B. Graves, Plasma Sources Sci. Technol. **14**, 273 (2005).

[21] C. Suzuki, K. Sasaki, , and K. Kadota, Journal of Applied Physics **82**, 5321 (1997).

[22] C. Suzuki, K. Sasaki, and K. Kadota, Jpn. J. Appl. Phys. Part 1 **37**, 5763 (1998).

[23] J.-P. Booth, Plasma Sources Sci. Technol. **8**, 249 (1999).

[24] J. P. Booth, G. Cunge, P. Chabert, and N. Sadeghi, Journal of Applied Physics **85**, 3097 (1999).

[25] K. Sasaki, H. Furukawa, K. Kadota, and C. Suzuki, Journal of Applied Physics **88**, 5585 (2000).

[26] H. Nakagawa *et al.*, Jpn. J. Appl. Phys. Part 1 **41**, 319 (2002).